JOURNAL OF PROPULSION AND POWER
Vol. 12, No. 4, July–August 1996

Numerical Analysis of a Ram Accelerator Employing Two-Phase Combustion

Richard Saurel*
Université de Provence, 13397 Marseille, France

A numerical investigation is carried out of the flowfield around a ram accelerator projectile running through a tube filled with a detonating gas laden with reactive solid particles. First, a mathematical model for the two-phase, chemically reactive flow is proposed. A total variation diminishing numerical scheme is employed, based on the resolution of two Riemann problems: a classical one for the gas phase, and a nonconventional one for the dispersed phase. Results are presented, first for a ram projectile flying at 6.7 km/s through an H_2/O_2/He mixture, and compared with recent data. Then, computations are made for the same conditions, but with the addition of solid hydrazine nitrate particles. It appears that the existence of sufficiently small particles improve the performance of the ram accelerator.

Nomenclature

A, B, C = coefficients in Arrhenius laws
a = rate constant in the combustion law for a particle
C_d = drag coefficient
C_v = specific heat at constant volume
c_i = concentration of species i
d_j^n = slopes along x at time t of conservative variables for element T_j
E = total energy
E_{chem} = reaction energy in the combustion of solid particles
e = internal energy
Fd = drag force
F_1 = component along the x direction of the vector of conservative fluxes
F_2 = component along the y direction of the vector of conservative fluxes
h = convection coefficient
h_i^0 = formation enthalpy of species i
k = rate constant of a chemical reaction
L = projectile length
$\dot{m}$ = mass production caused from particle combustion
N_p = number of particles per unit volume
Nu = Nusselt number
n = exponent in the combustion law of a solid particle
$\boldsymbol{n}$ = unit normal, pointing outwards of T_j, for a given segment
n_1, n_2 = components of vector $\boldsymbol{n}$
P = pressure
Pr = Prandtl number
P_0 = gas pressure before the passage of the ram projectile
Q = convective heat flux
R = gas constant
Re = Reynolds number
r_p = particle radius
S_j = area of element j
S_p = area of a particle
T = temperature
T_j = element, or cell j
T_0 = temperature before the passage of the ram projectile
$\boldsymbol{U}$ = vector of conservative variables
u = z component of the velocity
v = r component of the velocity
W = molar mass
W_R = solution of the exact Riemann problem
X = molar fraction
Y = mass fraction
α = volume fraction
Δt = time step
δ_j^n = slopes along y at time t of conservative variables for element T_j
δT_j = contour of element T_j
$\delta T_j \cap \delta T_{jk}$ = interface between elements T_j and T_{jk}
λ = thermal conductivity
μ = dynamic viscosity
ν = stoichiometric coefficient
ρ = density
ω_i = production rate of species i
ω_j = c.g. of element T_j

Subscripts

g = gas phase
j = index for specifying element j
p = particle phase

Space and Time Coordinates

r, z = cylindrical space coordinates
t = time
x, y = Cartesian space coordinates

Introduction

OBLIQUE shock waves may be used to initiate the combustion of a gas mixture to generate thrust. Recent studies on the subject have been motivated by the emergence of the ram accelerator, which is being used to accelerate a projectile to very high velocities, as well as by the new concept of oblique detonation wave engine (ODWE), which is being advocated for powering the U.S. National Aerospace Plane (NASP). The ram accelerator (Ramac, Fig. 1) was first developed by Hertzberg et al.[1,2] In this concept, a projectile is launched at a high velocity, with the help of a light-gas gun,

Received March 2, 1994; presented as Paper 94-2968 at the AIAA/ASME/SAE/ASEE 30th Joint Propulsion Conference and Exhibit, Indianapolis, IN, June 27–29, 1995; revision received Nov. 18, 1995; accepted for publication Feb. 21, 1996.

*Associate Professor. Institut Universitaire des Systèmes Thermiques Industriels.

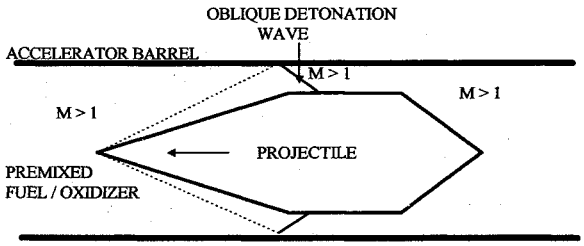

Fig. 1 Schematic of ram accelerator (adopted from Yungster et al.[6]).

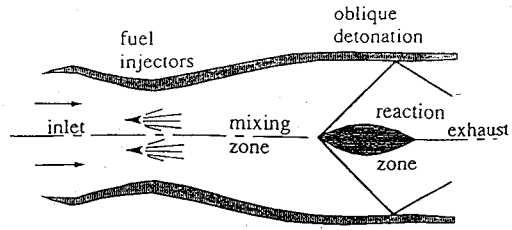

Fig. 2 Schematic of an oblique detonation wave engine (adopted from Powers et al.[5]).

into a tube filled with reacting gases. Because of the high velocity of the projectile, the leading and reflecting shock waves compress and heat the gases. When the increase in temperature is sufficient, the mixture of reacting gases ignites and combusts. Reaction occurs usually very fast and produces a combustion zone that seems to be a detonation wave. This results in a large increase of temperature and pressure. The resulting high pressure acts on the tail of the projectile producing a positive thrust. Under this thrust the projectile accelerates. Since its velocity increases, the leading and reflecting shock waves becomes stronger and the ignition and combustion of gases occurs sooner. This system is in theory a self-accelerating one.

There are several possible operating regimes of the Ramac: the subdetonating regime, in which the projectile velocity is lower than the gas detonation speed; the transdetonating regime, in which the two velocities are very close to each other; and the superdetonating one, symmetric to the subdetonating case. The projectile speed adopted hereafter corresponds to a superdetonating regime.

One of the main difficulties lies in the gas mixture one has to use in order to obtain good performances. Hertzberg et al. used a 16-m-long tube, 36-mm-i.d. filled, in its first three compartments, with gas mixtures of CH_4, O_2, N_2, and He in varying percentages at an initial pressure of 31 bars, and in the last compartment, with a mixture of $0.9CH_4 + 3O_2 + 5CO_2$ at 16 bars. A shock-initiated combustion process, which could accelerate a 70-g projectile from an initial velocity of 1200 m/s to a final speed of 2475 m/s (corresponding to Mach 8.4) was recorded.

Pressures of about 600 bars have been measured during the passage of the projectile. Part of the wave train is sketched in Fig. 1, the various expansion waves are not shown. The temperature dependence of the chemical reactions may lead to the formation of reaction zones, localized behind the attached shock, in the case of a fast projectile or behind the projectile base, at lower speeds. Among the applications being suggested, such a device might be used for direct orbital launching,[3] for hypervelocity impact studies or for hypersonic testing.

Recent theoretical and numerical studies[4,5] have been carried out to determine the flow in a ram accelerator or in an ODWE.[6,7] In these studies, the unsteady flow equations are solved, with a coupling of the gasdynamic and chemical–kinetic effects to reach steady state. Usually steady state was obtained using a relaxation numerical method for chemistry. We propose here a time-accurate numerical strategy similar to the one used by Li et al.[8]

Another ramjet-type propulsion device is known under the generic name of ODWE. The idea of using an ODWE with supersonic combustion for a high-speed aircraft was put forward as early as 1958 (Ref. 9). Its operation might be schematically described as in Fig. 2: a supersonic airstream is admitted in a duct. Fuel is injected as a liquid phase and the mixture reaches a ramp. The resulting shock wave compresses the gas and initiates combustion, generating a thrust force.

As shown in Fig. 2, the reacting gas mixture may be obtained by the vaporization of fuel droplets in the airstream. As a rule, downstream of the mixing zone, a purely gaseous mixture is produced; since all droplets have evaporated, one is led to the study of a reactive, but single-phase problem.[6,7] However, if one wishes to treat the problem in its entirety, i.e., from the air inlet to the jet exhaust, including the mixing and reaction zones, one is then compelled to study the problem of a two-phase, reacting flow.

The same approach can be envisaged for the ram accelerator: namely the motion of a projectile in a tube filled with detonating gas and reactive particles. Such a scheme should benefit from the additional energy of the particles. A similar idea has been pointed out by Cambier and Bogdanoff.[10] They proposed to add in the inner wall of the tube, a thin layer of solid high explosive to render the flow more energetic.

One might rightfully question the reason to render the setup even more complex by the addition of reacting particles, as the same gain in energy might be obtained either by increasing the initial gas density, or by using a more energetic gas mixture. The interest of a two-phase propulsion system resides in the specifics of the dynamics of the ignition and subsequent combustion of solid particles, by comparison with that of a gas mixture. Actually, the ignition of a gas mixture obeys Arrhenius' laws of branching reactions, and the subsequent combustion is governed by the same laws, exhibiting dependence on temperature only. By contrast, it is commonly accepted that solid particles ignite when reaching a certain temperature threshold, which is usually rather low (a value of 450 K is adopted in the present study). This ignition temperature is reached by the particles because of the various thermal exchanges taking place within the flow. On the other hand, the combustion dynamics of the particles are generally dependent on pressure only; this brings about a fundamental difference from the gaseous combustion.

These differences, which can be used to advantage by the designer, might, in principle, lead to the development of an improved propulsion system by bringing into play some new parameters: for example, the differences in the ignition dynamics of the gas and particles might bring about the existence of two reaction zones (the first for the gas and the second for the particles); if one could benefit from the presence of two reaction zones, one may improve the thrust or, alternately, initiate the combustion in certain zones that are more favorable to the overall performance.

The configuration envisaged in the present study is that described in the paper of Yungster.[6] A projectile made up of two 14-deg cones, connected by a cylindrical body. The projectile length is 19 cm and its radius 1.45 cm. The tube has a radius of 1.9 cm. The projectile travels at 6700 m/s (Mach 9) in the tube, which contains a mixture of $2H_2 + O_2 + 5He$ at 250 K and an initial pressure of 20 atm. Thus, one may compare our results with existing ones.[6]

Following this analysis, the case of a flow laden with a suspension of hydrazine nitrate particles will be taken up, and the previously-mentioned effects will be examined.

Analysis

A mathematical model is to be developed, depicting the re-

active, two-phase flow in a Ramac. To this end, certain assumptions are made:

1) The projectile is supposed to travel within the tube in a position that is symmetric to the tube axis and to its midplane. The symmetry with respect to the tube axis implies that no account is made for the presence of guiding winglets on the projectile. The problem is supposed to be two dimensional and axisymmetric.

2) The fluid is assumed to be inviscid and nonheat-conductive, except at the interfaces with the reactive particles.

3) The apparent density of the solid particles $[(1 - \alpha_g)\rho_p]$ is of the same order of magnitude as that of the gas. More specifically, if the suspension is a dilute one, it is reasonable to neglect the volume occupied by the particles. This assumption is valid in this study since few particles are added to the gaseous flow. Solid density is very high in front of gas density, and so void fraction α_g is closed to unity.

4) Particle size is greater than the mean free path of the gas molecules. Actually, spherical particles will be considered with diameters in the range 4–20 μm, much greater than the mean free path. This is necessary to allow the gas to be considered as a continuum at the particle scale.

5) Particles are initially of the same size.

6) We assume that no fragmentation or coalescence of the particles is taking place.

7) Interactions between particles are ignored.

8) The only force acting upon the particles is drag, and heat transfer takes place by convection only. Thus, the effect of wall radiation upon the particles is not taken into account. Also, radiation towards the gas is not considered.

9) Temperature inside a particle is supposed uniform. This is especially true since the particles are small.

10) Particles ignite after reaching a threshold temperature.

11) Particles slide along the walls.

12) Real-gas effects (equation of state differing from that of perfect gases) are not taken into account. These could be dealt with via the Riemann solvers developed by the author,[11] but would be costly in terms of CPU time, and not absolutely necessary for the present problem. The compressibility factor of the mixture at the highest pressure encountered here never exceeds 1.07, which is sufficiently close to unity to justify the ideal gas assumption.

13) The projectile does not to suffer any erosion and, therefore, its geometry is not changing.

By virtue of assumption 3, the void fraction, defined as α_g = gas volume/total volume, is close to unity. One may, therefore, neglect the volume taken by the particles and also its implication in the terms containing the pressure in the equations for the particle momentum and energy.[12] One is thus led to a simplified system of equations partially developed in previous work.[13–16]

Conservation of Mass:

$$\frac{\partial \alpha_g \rho_g}{\partial t} + \frac{\partial \alpha_g \rho_g u_g}{\partial z} + \frac{\partial \alpha_g \rho_g v_g}{\partial r} + \frac{\alpha_g \rho_g v_g}{r} = \dot{m} \tag{1}$$

$$\frac{\partial (1 - \alpha_g)\rho_p}{\partial t} + \frac{\partial (1 - \alpha_g)\rho_p u_p}{\partial z} + \frac{\partial (1 - \alpha_g)\rho_p v_p}{\partial r} + \frac{(1 - \alpha_g)\rho_p v_p}{r} = -\dot{m} \tag{2}$$

Conservation of Momentum:

$$\frac{\partial \alpha_g \rho_g u_g}{\partial t} + \frac{\partial (\alpha_g \rho_g u_g^2 + \alpha_g P)}{\partial z} + \frac{\partial (\alpha_g \rho_g u_g v_g)}{\partial r} + \frac{\alpha_g \rho_g u_g v_g}{r} = Fd_z + \dot{m} u_p \tag{3}$$

$$\frac{\partial \alpha_g \rho_g v_g}{\partial t} + \frac{\partial (\alpha_g \rho_g u_g v_g)}{\partial z} + \frac{\partial (\alpha_g \rho_g v_g^2 + \alpha_g P)}{\partial r} + \frac{\alpha_g \rho_g v_g^2}{r} = Fd_r + \dot{m} v_p \tag{4}$$

$$\frac{\partial (1 - \alpha_g)\rho_p u_p}{\partial t} + \frac{\partial [(1 - \alpha_g)\rho_p u_p^2]}{\partial z} + \frac{\partial [(1 - \alpha_g)\rho_p u_p v_p]}{\partial r} + \frac{(1 - \alpha_g)\rho_p u_p v_p}{r} = -Fd_z - \dot{m} u_p \tag{5}$$

$$\frac{\partial (1 - \alpha_g)\rho_p v_p}{\partial t} + \frac{\partial [(1 - \alpha_g)\rho_p u_p v_p]}{\partial z} + \frac{\partial [(1 - \alpha_g)\rho_p v_p^2]}{\partial r} + \frac{(1 - \alpha_g)\rho_p v_p^2}{r} = -Fd_r - \dot{m} v_p \tag{6}$$

Conservation of Energy:

$$\frac{\partial \alpha_g \rho_g E_g}{\partial t} + \frac{\partial u_g (\alpha_g \rho_g E_g + \alpha_g P)}{\partial z} + \frac{\partial v_g (\alpha_g \rho_g E_g + \alpha_g P)}{\partial r} + \frac{\alpha_g v_g (\rho_g E_g + P)}{r} = Fd_z u_p + Fd_r v_p + Q + \dot{m}[e_p + 0.5(v_p^2 + u_p^2)] \tag{7}$$

$$\frac{\partial (1 - \alpha_g)\rho_p e_p}{\partial t} + \frac{\partial [(1 - \alpha_g)\rho_p u_p e_p]}{\partial z} + \frac{\partial [(1 - \alpha_g)\rho_p v_p e_p]}{\partial r} + \frac{(1 - \alpha_g)\rho_p v_p e_p}{r} = -Q - \dot{m} e_p \tag{8}$$

The gas energy equation is written in terms of total energy while the particle energy equation is written in terms of internal energy. This equation is obtained subtracting kinetic energy equation to the total energy equation for the particles. The kinetic energy equation is obtained easily starting from the conservation momentum equation for the particles.

For the particles, the internal energy formulation is simpler and easier to solve numerically. This formulation is possible since there is no pressure in the particle equations. The system of equations for the particles remains conservative.

Conservation of Number Density of Particles

By virtue of assumption 6, the equation governing the evolution of this latter quantity is

$$\frac{\partial N_p}{\partial t} + \frac{\partial N_p u_p}{\partial z} + \frac{\partial N_p v_p}{\partial r} + \frac{N_p v_p}{r} = 0 \tag{9}$$

Knowledge of the number of particles per unit volume is necessary for expressing all two-phase coupling terms.[13,16] Particle number allows the calculation of particle diameter during combustion, which is necessary for the calculation of the Reynolds and Nusselt numbers, etc.

Conservation of the Chemical Species

The mixture of detonating gases through which the projectile is flying consists solely of H_2, O_2, and He, and the combustion products of the particles of $H_5N_3O_3$ are practically the same as those resulting from the combustion of the mixture H_2/O_2. The presence of burning solid propellant particles adds a new chemical species: N_2. Because of the high temperatures encountered, nitrogen may combine with oxygen. Because of the fact that the combustion of hydrazine particles brings about a supplementary amount of gas, consisting of H_2O, N_2, and

O_2, this contribution must be accounted for in the equations expressing the conservation of mass of the respective species:

$$\frac{\partial \alpha_g \rho_{H_2O}}{\partial t} + \frac{\partial \alpha_g \rho_{H_2O} u_g}{\partial z} + \frac{\partial \alpha_g \rho_{H_2O} v_g}{\partial r} + \frac{\alpha_g \rho_{H_2O} v_g}{r} = \omega_{H_2O} + \frac{5}{2} \frac{W_{H_2O}}{W_{H_5N_3O_3}} \dot{m} \tag{10}$$

$$\frac{\partial \alpha_g \rho_{N_2}}{\partial t} + \frac{\partial \alpha_g \rho_{N_2} u_g}{\partial z} + \frac{\partial \alpha_g \rho_{N_2} v_g}{\partial r} + \frac{\alpha_g \rho_{N_2} v_g}{r} = \omega_{N_2} + \frac{3}{2} \frac{W_{N_2}}{W_{H_5N_3O_3}} \dot{m} \tag{11}$$

$$\frac{\partial \alpha_g \rho_{O_2}}{\partial t} + \frac{\partial \alpha_g \rho_{O_2} u_g}{\partial z} + \frac{\partial \alpha_g \rho_{O_2} v_g}{\partial r} + \frac{\alpha_g \rho_{O_2} v_g}{r} = \omega_{O_2} + \frac{1}{4} \frac{W_{O_2}}{W_{H_5N_3O_3}} \dot{m} \tag{12}$$

$$\frac{\partial \alpha_g \rho_i}{\partial t} + \frac{\partial \alpha_g \rho_i u_g}{\partial z} + \frac{\partial \alpha_g \rho_i v_g}{\partial r} + \frac{\alpha_g \rho_i v_g}{r} = \omega_i \tag{13}$$

with i = OH, H, O, NO, N, H_2, HO_2, He.

The factors $\frac{5}{2}$, $\frac{3}{2}$, and $\frac{1}{4}$ are the stoichiometric coefficients figuring in the combustion equation of the hydrazine nitrate. The respective mass-production terms are from the combustion of the particles, whereas the ω_i terms are related to burning within the gas. These terms are discussed in the following.

Since the flow is very dilute in particle the void fraction α_g is closed to unity. For all equations for the gas phase one can eliminate this parameter. One can rewrite also all equations for the particles in terms of apparent density defined by $(1 - \alpha_g)\rho_p$. Therefore one recovers the notations used in a previous paper.[14]

Constitutive Laws for Two-Phase Exchanges

The gas-phase flow and the particle-phase flow are coupled by two-phase exchange terms.

Mass Exchange

The term $\dot{m}$ is because of the phase-change induced by the combustion of the particles. Specifically, the particle combustion mechanism is supposed to imply a single-stage irreversible reaction:

$$H_5N_3O_3 \rightarrow \tfrac{5}{2}H_2O + \tfrac{3}{2}N_2 + \tfrac{1}{4}O_2 \tag{14}$$

In this reaction we assume that hydrazine nitrate combustion produces only the species H_2O, N_2, and O_2 as stoichiometric processes. For this assumption we follow the remarks of Heuzé and Bauer[17] and Kamlet[18] about solid explosives. Moreover, it might be possible that water vapor (or nitrogen and oxygen) dissociates or chemically reacts because of the high temperature of the flow. These effects might create more numerous species. They are taken into account by the chemical gaseous production rates detailed in the 19 reactions chemical model that we will see in the next section.

The rate of reaction (14) being taken as a function uniquely of pressure, in accordance with the practice concerning solid propellants (Vieille's law). One gets,

$$\dot{m} = \frac{dr_p}{dt} S_p N_p \tag{15}$$

with $dr_p/dt = aP^n$, where a and n are experimentally determined and specific for the propellant in question [for hydrazine nitrate $a = 2 \times 10^{-7}$ m/(s·Pa^n) and $n = 0.85$], and $S_p = 4\pi r_p^2$.

Particle radius is obtained by the relation: $(1 - \alpha_g)\rho_p = N_p V_p \rho_p$, where ρ_p represents particle density assumed incompressible (ρ_p = 1600 kg/m^3 for hydrazine nitrate), V_p is the particle volume: $V_p = \frac{4}{3}\pi r_p^3$.

Momentum Exchanges

The main momentum coupling is because of the drag force. Fd_r and Fd_z represent the components along r and, respectively, z, of the drag force $\boldsymbol{Fd}$. This latter is taken from an experimental correlation:

$$\boldsymbol{Fd} = 6\pi r_p \mu (\boldsymbol{U}_p - \boldsymbol{U}_g) N_p C_d \tag{16}$$

with the drag coefficient[19] $C_d = 1 + 0.15Re^{0.687}$ for $Re < 1000$ and $C_d = 0.01833Re$ for $Re > 1000$; μ is the dynamic viscosity of the gas, while the Reynolds number is defined as

$$Re = 2\rho_g |\boldsymbol{U}_p - \boldsymbol{U}_g| r_p / \mu \tag{17}$$

The terms $\dot{m}u_p$ and $\dot{m}v_p$ are the expressions for momentum transfer caused from mass transfer.

Energy Exchanges

The term $Fd_z u_p + Fd_r v_p$ represents the work of the drag forces acting between gas and particles. Q is the convective heat transfer between gas and particles:

$$Q = S_p h (T_p - T_g) N_p \tag{18}$$

where $h = \lambda Nu/(2r_p)$. This is given as an experimental correlation: $Nu = 2 + 0.6Re^{0.55}Pr^{0.33}$ (Ref. 20).

Heat transfer and drag coefficient correlations have been determined in other experimental configurations rather than for the present application. But since, to the author's knowledge, no correlation exists for hypersonic flows, we have chosen often-used correlations. The term $\dot{m}e_p$ is the amount of energy gained by the gas because of particle combustion. The term $\dot{m}(u_p^2 + v_p^2)/2$ represents the kinetic energy transfer caused by mass transfer.

Constitutive Laws for Chemical Interactions

Recall first some complements and thermodynamic definitions. Total energy per unit mass for the gas expresses

$$E_g = \sum_{i=1}^{n} Y_i \int_{298}^{T} c_{vi}\, dT + e_i^{298} + \frac{1}{2}(u_g^2 + v_g^2) \tag{19}$$

where $Y_i = (\rho_i/\rho_g)$ the mass fraction for species i, c_{vi} is the specific heat at constant volume of species i. The expressions for the specific heats, as functions of temperature, for each of the chemical species, are given as regression polynomials, taken from the Chemkin thermodynamic database[21]:

$$\frac{c_{pi}}{R} = a_1 + a_2 T + a_3 T^2 + a_4 T^3 + a_5 T^4 \text{ and } c_{pi} - c_{vi} = R/W_i$$

The pressure P is obtained from the equation of state for a perfect gas:

$$P = \frac{\rho_g R T}{\bar{W}} \quad \text{with} \quad \bar{W} = 1 \Big/ \sum_{i=1}^{n} \frac{Y_i}{W_i}$$

where W_i is the molar mass of species i.

On another hand, the internal energy of the particles per unit mass e_p is defined following Powers et al.[16]:

$$e_p = c_{vp} T_p + E_{\text{chem}} \tag{20}$$

Table 1 Elemental reaction for the $H_2/O_2/N_2$ system

Species	Reactions	
1:H_2	1 = $H_2 + M \leftrightarrow 2H + M$,	2 = $O_2 + M \leftrightarrow 2O + M$
2:O_2	3 = $H_2O + M \leftrightarrow OH + H + M$,	4 = $OH + M \leftrightarrow O + H + M$
3:OH	5 = $H_2O + O \leftrightarrow 2OH$,	6 = $H_2O + H \leftrightarrow OH + H_2$
4:O	7 = $O_2 + H \leftrightarrow OH + O$,	8 = $H_2 + O \leftrightarrow OH + H$
5:H	9 = $H_2 + O_2 \leftrightarrow 2OH$,	10 = $HO_2 + M \leftrightarrow H + O_2 + M$
6:H_2O	11 = $H_2 + O_2 \leftrightarrow H + HO_2$,	12 = $2\,OH \leftrightarrow H + HO_2$
7:He	13 = $H_2O + O \leftrightarrow H + HO_2$,	14 = $OH + O_2 \leftrightarrow O + HO_2$
8:HO_2	15 = $H_2O + O_2 \leftrightarrow OH + HO_2$,	16 = $H_2O + OH \leftrightarrow H_2 + HO_2$
9:N_2	17 = $N_2 + O \leftrightarrow N + NO$	
10:N	18 = $H + NO \leftrightarrow OH + N$	
11:NO	19 = $O + NO \leftrightarrow N + O_2$	

Table 2 Reactions rates[a]

Reaction no.	Forward rate constant			Reverse rate constant		
	A	B	C, K	A	B	C, K
1	5.5×10^{18}	−1	51,987	1.8×10^{18}	−1	0
2	7.2×10^{13}	−1	59,340	4.0×10^{17}	−1	0
3	5.2×10^{21}	−1.5	59,386	4.4×10^{20}	−1.5	0
4	8.5×10^{18}	−1	50,830	7.1×10^{16}	−1	0
5	5.8×10^{13}	0	9,059	5.3×10^{12}	0	503
6	8.4×10^{13}	0	10,116	2.0×10^{13}	0	2,600
7	2.2×10^{14}	0	8,455	1.5×10^{13}	0	0
8	7.5×10^{13}	0	5,586	3.0×10^{13}	0	4,429
9	1.7×10^{13}	0	24,232	5.7×10^{11}	0	14,922
10	1.7×10^{16}	0	23,100	1.1×10^{16}	0	−440
11	1.9×10^{13}	0	24,100	1.3×10^{13}	0	0
12	1.7×10^{11}	0.5	21,137	6.0×10^{13}	0	0
13	5.8×10^{11}	0.5	28,686	3.0×10^{13}	0	0
14	3.7×10^{11}	0.64	27,840	1.0×10^{13}	0	0
15	2.0×10^{11}	0.5	36,296	1.2×10^{13}	0	0
16	1.2×10^{12}	0.21	39,815	1.7×10^{13}	0	12,582
17	5.0×10^{13}	0	37,940	1.1×10^{13}	0	0
18	1.7×10^{14}	0	24,500	4.5×10^{13}	0	0
19	2.4×10^{11}	0.5	19,200	1.0×10^{12}	0.5	3,120

where c_{vp} is the specific heat of the particles (c_{vp} = 1493 J/kg·K), E_{chem} is the chemical energy of the propellant (3.7×10^6 J/Kg for $H_5N_3O_3$).

The combustion model retained includes 19 reversible reactions, involving 11 chemical species; helium is assumed inert (Table 1). Reactions (1–16) are taken from Evans and Schexnayder,[22] who studied a problem of supersonic combustion. Reactions (17–19) are taken from Kee et al.[21] where a reduced kinetic model is proposed for the system $H_2/O_2/N_2$. As will be shown, the 19-equation model can be reduced to an 8-equation model for the system H_2/O_2, however, certain small differences may then be found, irrelevant in practice, but displaying the sensitivity of the results to the chemical modeling.

The direct rate constants for each j reaction are given as terms of pseudo-Arrhenius laws (Table 2):

$$k_{fj} = AT^B \exp[-(C/T)] \tag{21}$$

The reverse rate constants are similarly defined.

The chemical production terms of each i species are deduced from the direct and inverse reaction rates, k_{fj} and k_{bj}, and the concentrations of the species:

$$\omega_i = W_i \sum_{j=1}^{J} \nu_{ji} q_j \tag{22}$$

The production rate q_j is obtained as the difference between the direct and inverse rates:

$$q_j = k_{fj} \prod_{i=1}^{n} (X_i)^{\nu'_{ji}} - k_{bj} \prod_{i=1}^{n} (X_i)^{\nu''_{ji}} \tag{23}$$

where (X_i) is the molar concentration of species i.

Numerical Procedure

To our knowledge the resolution of chemically reacting and two-phase flows is rather rare. Among the trials of resolution of problems where two-phase and reactive effects are coupled one can cite the work of Hayashi et al.[23] using a first-order accuracy scheme for the particle phase equations. We propose here an extension for reactive flows of a scheme[14] for the resolution of two-phase flows. This scheme is a second-order Godunov type, over unstructured meshes. The new extension to reactive flows is based on original ideas of Oran and Boris.[24]

The system to be solved consists of Eqs. (1–13) and is rather complex. It should, therefore, be useful if one could split the overall system into several smaller subsystems. Equations (1), (3), (4), and (7) represent a subsystem for the gas phase (system S1), whereas Eqs. (2), (5), (6), (8), and (9) represent the subsystem for the dispersed phase (system S2); finally, Eqs. (10–13) are the equations governing the evolution of the chemical species (system S3).

Hereafter the principles of the method will be recalled and the extension to chemically reacting flows detailed.

1) The overall system is split into systems S1, S2, and S3; this can be done if one takes only their homogenous parts. Actually, by reason of assumption 3, pressure is absent from particle momentum and energy equations. If one writes the equations in terms of apparent density, it appears clearly that the homogenous parts of systems S1 and S2 are fully uncoupled (the same is true for systems S2 and S3).

On the other hand, it is admitted, as a customary procedure, to uncouple the fluid dynamics (S1) from the chemistry (S3). Each time step will then comprise a dynamic substep, with frozen chemistry, followed by a chemistry step (convection of species and reaction). Systems S1, S2, and S3 being thus con-

sidered as independent, one proceeds by successively solving their homogenous parts.

2) Solution of the homogenous part of system S1. This system is stricly hyperbolic, its characteristic directions are well known: u_g, $u_g \pm c_g$ (c_g gas sound speed). This step is carried out by a classical scheme, which will be explained in the following. It consists of a second-order Godunov scheme, employing an exact and fast Riemann solver, following the strategy put forward by Gottlieb and Groth.[25]

3) Solution of the homogenous part of system S2. The same approach is followed as for system S1, with S2 also being hyperbolic. But it admits a single degenerated characteristic direction: u_p. Traditionally, other authors are using, when solving equations of the type S2, either centered finite difference schemes, following MacCormack[26] (see e.g., Refs. 27 and 28), or a donor-cell setup, first-order accurate[29]; however, we wish to retain second-order accuracy in the solution of S2. By considering a new Riemann problem for system S2, and including its solution in the Godunov-type scheme, one accomplishes easily the extension to second order. Therefore, the same numerical scheme will be employed both for systems S1 and S2, but with a classical Riemann solver for the gasdynamics system S1, and a new Riemann solver for the multivaluated system S2. Full details about the Riemann solver may be found in Ref. 14.

4) Solution of the homogenous part of system S3. Once the gasdynamic flowfield is determined, through the solution of system S1, one may proceed to solve system S3. So that this solution also be accurate to second order, certain precautions have to be taken at the predictor step.

5) Coupling of systems S1, S2, S3. This is done via the two-phase interaction terms and the source terms coming from the chemical interactions. One is then led to ordinary differential equations (ODE), in which the source terms may be stiff. This is a well-known problem in the study of reactive flows, where the chemistry is governed by Arrhenius-type laws. One must then employ an accurate, robust, fast, and convenient ODE solver. The variable coefficient ODE (DVODE) solver for differential equations[30] fulfills these requirements. This solver is implicit, when the problem is not excessively stiff and does not require the analytical derivation of the Jacobians, while being explicit in stiff regions. The solution procedure is shifted automatically, depending on the stiffness of the problem.

Now the main steps of the general procedure will be summarized for the solution of systems S1, S2, and S3. This scheme makes use of the main ideas of Van Leer.[31] Although not strictly necessary for the present application, for the sake of generality, the main steps will be presented following an unstructured mesh approach.

In an unstructured mesh, consider a cell T_j inside which the solution is supposed to be a monotonous function, this function will be defined by a mean value U_j^n and two slopes: d_j^n in the x direction and δ_j^n in the y direction. Let $I(j)$ be the manifold

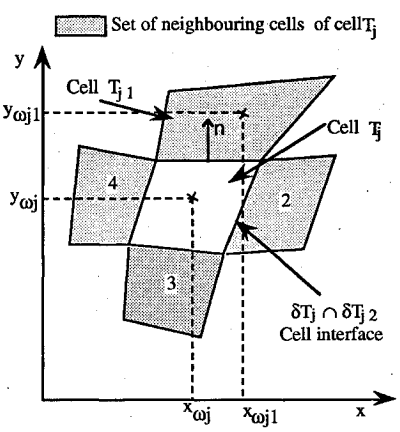

Fig. 3 Elements of a nonstructured grid.

neighbors of T_j. The contour of element T_j (Fig. 3) will be denoted by δT_j. Let ω_j and ω_{j1} be the centers of gravity of T_j and T_{ji}, and denote their coordinates by $x_{\omega j}$ and $y_{\omega j}$ ($x_{\omega j1}$ and $y_{\omega j1}$).

The homogenous parts of systems S1 and S2 may be written in vector form [Eq. (24)]. The following is valid for both systems S1 and S2; only the solution of the Riemann problem differs. For system S3 the scheme will have to be slightly modified.

With the axisymmetric part being treated as a source term, one is reduced to a two-dimensional problem, governed by Eq. (24) [F_1 and F_2 represent the eulerian conservative fluxes given by the set of Eqs. (1–13)]:

$$\frac{\partial U}{\partial t} + \frac{\partial F_1}{\partial x} + \frac{\partial F_2}{\partial y} = 0 \tag{24}$$

The first step (predictor) consists of computing the values of $U_{\delta T_j}^{n+1/2}$ as seen from inside the element contour δT_j (e.g., $\delta T_j \cap \delta T_{j1}$). One obtains

$$U_{\delta T_j \cap \delta T_{j1}}^{n+1/2} = U_j^n + \frac{1}{2} d_j^n (x_{\omega j} - x_{\omega j1}) + \frac{1}{2} \delta_j^n (y_{\omega j} - y_{\omega j1}) - \frac{\Delta t}{2} \frac{\partial F_1(U_j^n)}{\partial U} d_j^n - \frac{\Delta t}{2} \frac{\partial F_2(U_j^n)}{\partial U} \delta_j^n$$

One must compute the fluxes of the various variables across the interface $\delta T_j \cap \delta T_{j1}$, along the normal to this segment: then, one is led to solving a set of one-dimensional Riemann problems. Let $\boldsymbol{n}$ be the normal to the segment $\delta T_j \cap \delta T_{j1}$, pointing outwards of T_j. Define also the vector $V_n(\boldsymbol{u}) = (\rho, \rho \boldsymbol{u} \cdot \boldsymbol{n}, \rho e)^T$, associated to the vector $\boldsymbol{U}$, with $\boldsymbol{u} = (u, v)^T$. The vector $V_n(\boldsymbol{u})$, which will allow the computation of the fluxes along the normal, is a solution of the Riemann problem (gas or particles), computed at the interface between two cells:

$$V_{\delta T_j \cap \delta T_{j1}}^{n+1/2} = W_R^{G,P}[0, V_{n\delta T_j \cap \delta T_{j1}}(U_{\delta T_j \cap \delta T_{j1}}^{n+1/2}), V_{n\delta T_j \cap \delta T_{j1}}(U_{\delta T_{j1} \cap \delta T_j}^{n+1/2})]$$

$W_R^{G,P}$ denotes the solution of the exact Riemann problem for the gas or the particles.

One may now apply the conservation law: recalling that the F_i are computed at the middle of each face and are supposed to be constant along each segment, one gets, denoted by n_i^* the (nonunit) normal to face i:

$$\frac{U_j^{n+1} - U_j^n}{\Delta t} + \frac{1}{S_{T_j}} \sum_{k=1}^{I(j)} [F_1(V_{\delta T_j \cap \delta T_{jk}}^{n+1/2}) n_{1\delta T_j \cap \delta T_{jk}}^* + F_2(V_{\delta T_j \cap \delta T_{jk}}^{n+1/2}) n_{2\delta T_j \cap \delta T_{jk}}^*] = 0$$

It remains to compute the slopes over the cells; to this purpose, the total variation diminishing (TVD) concept is applied. The flux limiter developed hereafter is, actually, the minmod limiter.

If the quantities $(U_j^{n+1} - U_k^n)/(x_{\omega j} - x_{\omega k})$ for $k = j1, \ldots, j4$ have the same sign, then

$$d_j^{n+1} = \text{sign}\left(\frac{U_j^{n+1} - U_{j1}^n}{x_{\omega j} - x_{\omega j1}}\right) \min_{k=j1,\ldots,j4} \left|\frac{U_j^{n+1} - U_k^n}{x_{\omega j} - x_{\omega k}}\right|$$

else $d_j^{n+1} = 0$

In the same way, the gradients δ_j^n are computed along the direction y.

What remains to be done is to detail the necessary modifications of the scheme to be able to treat the system S3. The homogenous part of each of the equations of S3 is of the form

$$\frac{\partial \rho_i}{\partial t} + \frac{\partial \rho_i u_g}{\partial x} + \frac{\partial \rho_i v_g}{\partial y} = 0$$

To preserve second-order accuracy to this equation, the quantity ρ_i has to be a piecewise linear function. Now, since $\rho_i = \alpha_g \rho_g Y_i$, and since $\alpha_g \rho_g$ is piecewise linear, it suffices that Y_i be piecewise constant. If Y_{iT_j} is a constant over the cell T_j, then it will have the same value at the bounds of the interval $\delta T_j \cap \delta T_{jk}$. The value of ρ_i over the bounds of cell T_j, at the predictor step, is now readily obtained:

$$\rho_{i\delta T_j \cap \delta T_{j1}}^{n+1/2} = \rho_{g\delta T_j \cap \delta T_{j1}}^{n+1/2} Y_i T_j$$

or in terms of conservative variables

$$\rho_{i\delta T_j \cap \delta T_{j1}}^{n+1/2} = \rho_{g\delta T_j \cap \delta T_{j1}}^{n+1/2} \rho_i^n T_j / \alpha_g \rho_g^n T_j$$

Therefore, it is not necessary to compute the Jacobians of system S3 at the predictor step. Since the solution of the Riemann problem at the interfaces had already been determined, the components of the velocity vector for the gas are known, at the interfaces $\delta T_j \cap \delta T_{jk}$. The conservation law is thus reduced to a simple donor-cell-type law, depending on the sign of the velocity with respect to the outward-pointing normal (from element T_j) of the face $\delta T_j \cap \delta T_{jk}$.

Boundary Conditions

The grid, dimension, and computational domain may be represented schematically as in Fig. 4. At boundary B_1 the gas flow is supersonic. On the other hand, the particle equations forbid any information to propagate upstream. Therefore, one has to impose, on B_1, all of the gas and particle magnitudes. On B_2, for the gas phase, classical wall conditions are imposed ($\boldsymbol{V} \cdot \boldsymbol{n} = 0$). On B_3, one applies absorption conditions for both the gas and particles ($\partial \boldsymbol{V}/\partial \boldsymbol{n} = 0$ and $\partial \rho/\partial \boldsymbol{n} = 0$). This type of boundary condition is detailed in a previous paper[14] for the particle phase system of equations. Regarding the gas phase, this formulation does not mean that gradients are zero on the meshes at B_3 but only on the mesh interface B_3. On B_4 one applies symmetry conditions ($\boldsymbol{V} \cdot \boldsymbol{n} = 0$). On B_5, one applies classical wall conditions for the gas. The problem is to develop realistic boundary conditions for the particles on B_5, but also on B_2. The question of wall–particle interactions is a complex one, and is still with us. Recent works[32] emphasize that the particle–wall interaction depends upon numerous parameters, including the impacting particle velocities and the state of the surface. One may expect that, at hypervelocities such as envisaged in our application, the particles would show a tendency to burst when striking the wall, and may spontaneously detonate under the impact, or encrust upon the projectile and rapidly erode it. To avoid having to deal with such problems, one considers that the particles come into the flow uniquely through the annular zone between the maximum radius of the projectile and the tube wall. Direct impacts are avoided and one may reasonably suppose that the particles will slide along the walls. This would imply that the physical layout keep the particles close to the tube wall and then release them at the passage of the projectile. Particles sticking to the wall are not evident, but one can imagine achieving this, for example, by electrostatic means.

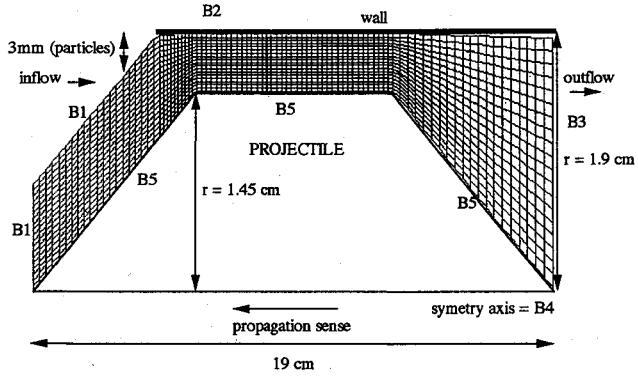

Fig. 4 Representation of the various boundary conditions and dimensions.

Code Versatility

The code developed may be applied either to two-phase, diluted flows, or to reactive systems. It may be used in conjunction with unstructured meshes, generated by any standard finite element mesh generator, and therefore, diversified geometries may be handled. Because of the fact that the numerical method is almost the same for dealing with the equations for the gasdynamics, particle dynamics, and chemical species, the development of the code is rendered easier and the resulting product is compact. To deal with the problems to be discussed hereafter, only 1500 Fortran lines were necessary. Problems involving 10,000 cells may be solved using only 8 Mbytes of RAM, while the CPU time for the costlier applications is about 4×10^{-2} s/point/iteration on a SUN-SPARC 10 machine (135 Mips–22 Mflops). For the applications to be presented, about 2000 cells were retained; the convergence for two-phase, reactive flows is obtained after 1000 time steps, requiring 20 hours CPU.

Results

Before considering applying the computer code to the full case of two-phase, chemically reactive media, one must validate the code. Since 1988, numerous experimental studies on the Ramac have been carried out in the U.S. (Univ. of Washington) and in France (French–German Research Institute, Saint Louis; see Giraud et al.[33]). Experimentally, the superdetonative regime is difficult to reach. It has also been demonstrated that the experimental reality is three dimensional. Moreover, flow visualization and diagnostic measurements are not easy inside a Ramac tube; therefore, the mapping of the flow is still uncertain, although great progress has been recently achieved.[34] For the time being, it seems difficult to attempt validating a code with reference to experimental results.

Good-quality simulations have already been performed, which can be considered as a reference for comparison of our results. We intend therefore, to compare our simulations with the data of Yungster et al.[6] for the cases in which only the gas is reactive. We consider that the two-phase part of our code has already been validated.[28]

Yungster et al.[6] have published data of a simulation for a projectile traveling at 6.7 km/s in a tube filled with a mixture of $2H_2 + O_2 + 5He$ at 20 atm and 250 K. The kinetic model employed by Yungster involved eight reactions, i.e., it took account of reactions 1–8 in Table 1. For the same projectile geometry, with the same kinetic model, but with the numerical procedure developed previously, our results are shown in Fig. 5. For clarity, an expansion factor of 5 was applied to the radial scale. The position of the combustion wave is clearly visible, at the nondimensional abscissa of 0.33. Yungster finds this position at 0.4, and the combustion zone appears to be more curved than in our results. These slight differences have encouraged us to try a more complete chemical model (the first 16 reactions of Table 1). With this, the position of the combustion zone shifts to 0.45, but the detonation remains plane (Fig. 6). The effects of the gridding were then investigated. The grid employed by Yungster is not reported; we have tried grids of up to 7000 cells, instead of 2000. Results were exactly the same: this leads us to think that numerical diffusion is not responsible for the differences. In fact, the main influence is produced by the chemical model. The branching reactions, and those which close the chemical system, require the intervention of a third body. Neither Yungster et al.,[6] nor Evans and Schexnayder[22] report on the nature and effectiveness of the third body considered. In our analysis, we have taken helium as third body, which is inert. However, it is obvious that any other choice would have led to slightly different results, since the

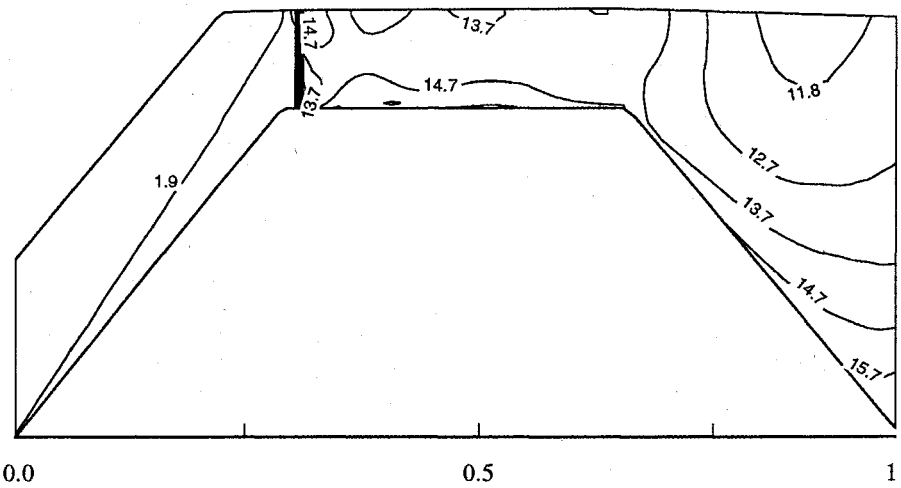

Fig. 5 Nondimensional T/T_0 temperature contours around the Ramac projectile, obtained with the 8-equation kinetic model.

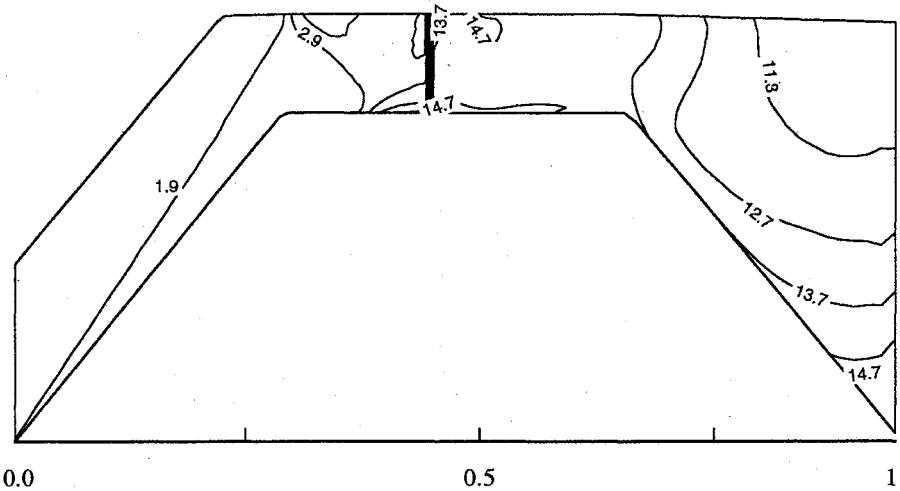

Fig. 6 Nondimensional T/T_0 temperature contours around the Ramac projectile, obtained with the 16-equation kinetic model.

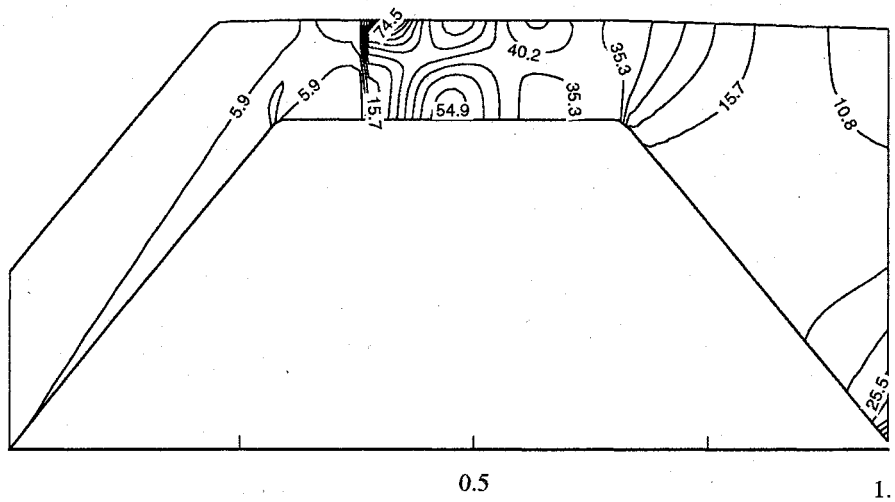

Fig. 7 Nondimensional P/P_0 pressure contours around the Ramac projectile flying through a mixture of H_2/O_2/He seeded with hydrazine particles.

branching reactions, which bring into play this third body, determine the position of the reaction zone.

To conclude, notwithstanding the slight discrepancies in the position of the reaction zone, one may say that, qualitatively, and even quantitatively, our results are quite close to Yungster's. We shall, therefore, admit that the reactive part of the code is sufficiently trustworthy to proceed with the study of the coupling with two-phase phenomena.

As remarked at the start of this section, the effects induced by the presence of reactive particles within the flow may open up a whole realm of interesting developments for engines based on oblique detonation waves. The same geometrical Ra-

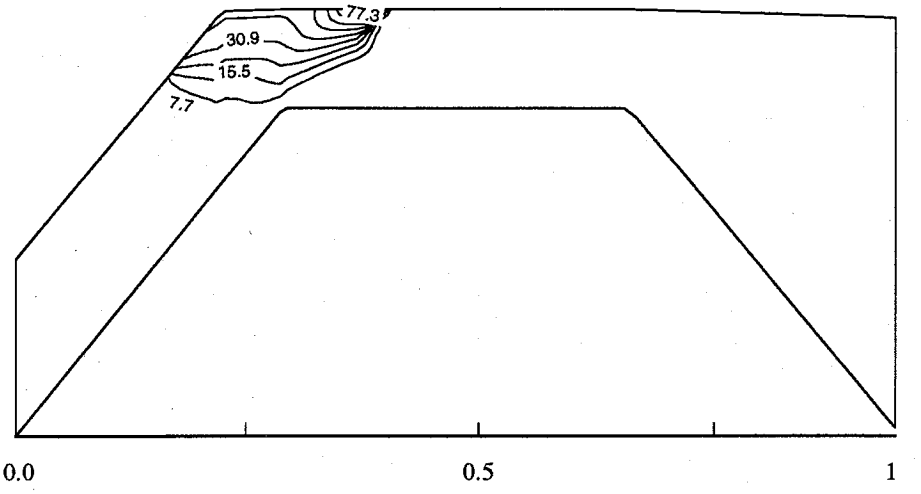

Fig. 8 Contours of the apparent particle density around a Ramac projectile flying through a mixture of H_2/O_2/He seeded with hydrazine particles.

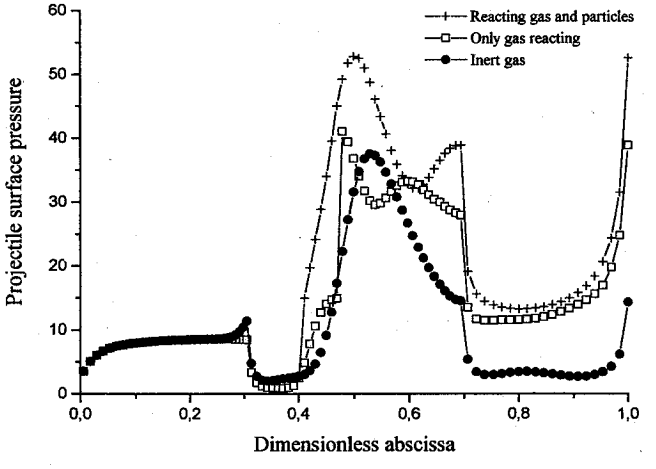

Fig. 9 Dimensionless pressure distribution along the projectile surface.

mac configuration will again be retained. For the chemistry, the 19-equation model is used. The flow is seeded with 4-μm-diam hydrazine particles, with an apparent injection density of 40 kg/m^3. The particles are injected in the direction of the flow, initially localized in a space comprised between the radius of 1.6 cm and the tube wall, simulating that the particles are sticking to the wall. This is done to avoid (conceptually) direct particle impacts upon the projectile, with the drawbacks already mentioned. Figure 7 shows the steady-state pressure field, while Fig. 8 represents the particle density field.

In Fig. 8 the particles, having been injected in a zone of 3 mm width, are found close to the wall after the passage of the shock. This is because of the fact that the particles being considered have a low dynamic inertia, and are strongly entrained by the gas being deflected by the projectile nose. Downstream of the oblique shock attached to the nose, the gas possesses a radial velocity component of up to 700 m/s. This is sufficient to carry the particles toward the tube wall where they remain because of their inertia. The particles react quite rapidly as, at the nondimensional abscissa of 0.4, that there are no particles left into the flow; they have, therefore, released their combustion energy into the gas. This translates into a violent pressure increase, 75 times the initial pressure of the medium through which the ram projectile is flying (Fig. 7), by comparison with only a 50-fold increase in the absence of particles.[6] Figure 9 illustrates the performance gain on the Ramac. The pressure profile on the projectile surface is represented. The thrust is equal to the sum of the pressure forces acting upon this surface. To get positive net thrust, the area under the pressure curve, comprised between abscissa 0.7 and 1.0, must be greater than that between 0.0 and 0.3 (the nose). The first curve represents the pressure generated in the inert two-phase case, i.e., without any chemical reactions in the gas. The net thrust is negative in this case. The second curve corresponds to the case when only the gas reacts; there is a positive net thrust now. The last curve is for both gas and particles reacting: the thrust gain is noticeable by comparison with the former case. As previously pointed out, the reactivity and ignition susceptibility of the particles depend on their size. For particles smaller than 4 μm, quite similar results have been obtained; whereas if the diameter is increased to 6 μm, ignition takes place downstream the nondimensional abscissa 0.7, where a strong centered expansion is present. Because of this fact, the combustion velocity of the particles, being a function of the pressure, is diminished, and the thrust is reduced. For particles larger than 10 μm, ignition is no longer seen within the computational domain; this produces a loss of energy of the gas and a fall in pressure at the projectile wall. This is because of the energy lost by the gas to the particles, which is no longer restored into the gas flow.

Conclusions

The effects of the presence of reactive gas particles within the flow in a Ramac have been explored. A two-phase reactive model for the flow type being investigated has first been established. Then, a TVD scheme has been developed for the numerical treatment of the manifold of equations.

Some computations of one- and two-dimensional reactive flows, in the absence of particles, are carried out, for a H_2/O_2/He mixture; thereafter, hydrazine nitrate particles are injected in this gas. The resulting flow becomes two-phase and more energetic. If the particles are initially injected in the vicinity of the tube wall, later direct impacts with the projectile nose are avoided, and a significant thrust gain is displayed. A new development of this propulsion system is envisaged, involving an addition of solid propellant particles to the initial reactive gas mixture. Favorable effects are expected with sufficiently small particles.

Acknowledgments

The author would like to acknowledge P. Barry Butler for his encouragement during this work, and my colleague Eric Daniel for much helpful advice.

References

[1]Herzberg, A., Bruckner, A. P., and Bogdanoff, D. W., "Ram Accelerator: A New Chemical Method for Accelerating Projectiles to

Ultrahigh Velocities," *AIAA Journal*, Vol. 26, No. 2, 1988, pp. 195–203.

[2]Herzberg, A., Bruckner, A. P., and Knowlan, C., "Experimental Investigation of Ram Accelerator Propulsion Modes," *Shock Waves*, Vol. 1, No. 1, 1991, pp. 17–25.

[3]Bogdanoff, D. W., "Ram Accelerator Direct Space Launch System—New Concepts," *Journal of Propulsion and Power*, Vol. 8, No. 2, 1992, pp. 481–490.

[4]Brackett, D. C., and Bogdanoff, D. W., "Computational Investigation of Oblique Detonation Ramjet-in-Tube Concepts," *Journal of Propulsion and Power*, Vol. 5, No. 2, 1989, pp. 276–281.

[5]Grismer, M. J., and Powers, J., "Calculation for Steady Propagation of a Generic Ram Accelerator Configuration," *Journal of Propulsion and Power*, Vol. 11, No. 1, 1995, pp. 105–111.

[6]Yungster, S., Eberhardt, S., and Bruckner, A. P., "Numerical Simulation of Hypervelocity Projectiles in Detonable Gases," *AIAA Journal*, Vol. 29, No. 2, 1991, pp. 187–199.

[7]Yungster, S., and Bruckner, A. P., "Computational Studies of a Superdetonative Ram Accelerator Mode," *Journal of Propulsion and Power*, Vol. 8, No. 2, 1992, pp. 457–463.

[8]Li, C., Kailasonath, K., Oran, E. S., Landsberg, M., and Boris, J. P., "Dynamics of Oblique Detonation in Ram Accelerator," *Shock Waves*, Vol. 5, Nos. 1,2, 1995, pp. 97–101.

[9]Dunlap, R., Brehm, R. L., and Nichols, J. A., "A Preliminary Study of the Application of Steady State Detonation Combustion to a Reaction Engine," *Jet Propulsion*, Vol. 28, No. 7, 1958, pp. 451–458.

[10]Cambier, J. L., and Bogdanoff, D. W., "Ram Acceleration from a Two Phase Detonative System," *Proceedings of the First International RAMAC Workshop*, Saint Louis, France, 1993.

[11]Saurel, R., Larini, M., and Loraud, J. C., "Exact and Approximate Riemann Solvers for Real Gases," *Journal of Computational Physics*, Vol. 112, 1994, pp. 126–137.

[12]Rudinger, G., "Some Effect of Finite Particle Volume on the Dynamics of Gas-Particle Mixtures," *AIAA Journal*, Vol. 3, No. 7, 1965, pp. 1217–1222.

[13]Saurel, R., Loraud, J. C., and Larini, M., "Optimization of a Pyrotechnic Igniter by the Release of Pyrotechnic Particles," *Shock Waves*, Vol. 1, No. 2, 1991, pp. 121–133.

[14]Saurel, R., Daniel, E., and Loraud, J. C., "Two-Phase Flows: Second Order Schemes and Boundary Conditions," *AIAA Journal*, Vol. 32, No. 6, 1994, pp. 1214–1221.

[15]Ishii, R., Umeda, Y., and Yuhi, M., "Numerical Analysis of Gas-Particle Two-Phase Flows," *Journal of Fluid Mechanics*, Vol. 203, 1989, pp. 475–515.

[16]Powers, J. M., Stewart, D. S., and Krier, H. "Theory of Two-Phase Detonations Part I: Modeling," *Combustion and Flame*, Vol. 80, 1990, pp. 264–279.

[17]Heuze, O., and Bauer, P., "A Simple Method for the Calculation of the Detonation Properties of CHNO Explosives," *Proceedings of the International Symposium on High Dynamic Pressures* (La Grande Motte, France), Ed. AFP; La Ferte St. Aubin, France, 1989, pp. 225–232.

[18]Kamlet, M. J., and Ablard, J. E., "Chemistry of Detonations, 2. Buffered Equilibria," *Journal of Chemical Physics*, Vol. 48, No. 1, 1968, pp. 36–42.

[19]Rowe, P. N., "Drag Forces in a Hydraulic Model of a Fluidized Bed. Part II," *Transactions of the Institution of Chemical Engineers*, Vol. 39, 1961, pp. 175–180.

[20]Yuen, M. C., and Chen, L. W., "Heat Transfer Measurements of Evaporating Liquid Droplets," *International Journal of Heat and Mass Transfer*, Vol. 21, 1977, pp. 537–542.

[21]Kee, R. J., Rupley, F. M., and Miller, J. A., "CHEMKIN II: A Fortran Chemical Kinetics Package for the Analysis of Gas Phase Chemical Kinetics," Sandia National Labs., SAND89-8009B, UC-706, 1993.

[22]Evans, J. S., and Schexnayder, C. J., "Influence of Chemical Kinetics and Unmixedness on Burning in Supersonic Hydrogen Flames," *AIAA Journal*, Vol. 18, No. 2, 1980, pp. 188–193.

[23]Hayashi, A. K., Makida, M., and Fujiwara, T., "Numerical Study of Hexane Spray Jet Combustion," *Archivu Combustion*, Vol. 14, No. 3, 1994, pp. 37–47.

[24]Oran, E., and Boris, J. P., *Numerical Simulation of Reactive Flow*, Elsevier, New York, 1987, pp. 314–357.

[25]Gottlieb, J. J., and Groth, C. P. T., "Assessment of Riemann Solvers for Unsteady One-Dimensional Inviscid Flows of Perfect Gases," *Journal of Computational Physics*, Vol. 78, 1988, pp. 437–458.

[26]MacCormack, R. W., "The Effect of Viscosity in Hypervelocity Impact Cratering," AIAA Paper 69-354, July 1969.

[27]Chang, I. S., "One and Two-Phase Nozzle Flows," *AIAA Journal*, Vol. 18, No. 2, 1980, pp. 1455–1461.

[28]Daniel, E., Saurel, R., and Loraud, J. C., "A Comparison Between Finite Difference and Finite Volume Formulation for Computation of Two-Phase Flows," AIAA Paper 93-2346, July 1993.

[29]Yang, X., Eidelman, S., and Lottati, I., "Computation of Shock Wave Reflection and Diffraction over a Semicircular Cylinder in a Dusty Gas," AIAA Paper 93-2940, July 1993.

[30]Brown, P. N., Byrne, G. D., and Hindmarsh, A. C., "VODE: A Variable Coefficient ODE Solver," *SIAM Journal on Scientific and Statistical Computing*, Vol. 10, 1989, pp. 1038–1051.

[31]Van Leer, B., "Toward the Ultimate Conservative Scheme V. A Second Order Sequel to Godunov's Method," *Journal of Computational Physics*, Vol. 32, 1979, pp. 101–136.

[32]Sommerfeld, M., "Modelling of Particle-Wall Collisions in Confined Gas-Particle Flows," *International Journal of Multiphase Flows*, Vol. 18, No. 6, 1992, pp. 905–926.

[33]Giraud, M., Legendre, J. F, and Simon, G., "Ram Accelerator at ISL. First Experiments in 90mm Caliber," Rept. ISL/CO 23191 ISL, Saint Louis, France, 1991.

[34]Hinkey, J. B., Burnham, E. A., and Bruckner, A. P., "High Spatial Resolution Measurements of Ram Accelerators Gas Dynamic Phenomena," AIAA Paper 94-3244, July 1992.